Published OnlineFirst April 8, 2020; DOI: 10.1158/1078-0432.CCR-19-2777

Repotrectinib Exhibits Potent Antitumor Activity in Treatment-Naïve and Solvent-Front–Mutant ROS1-Rearranged Non–Small Cell Lung Cancer

Mi Ran Yun[1,2], Dong Hwi Kim[1], Seok-Young Kim[1], Hyeong-Seok Joo[1], You Won Lee[2], Hun Mi Choi[2], Chae Won Park[2], Seong Gu Heo[3], Han Na Kang[1,2], Sung Sook Lee[4], Adam J. Schoenfeld[5], Alexander Drilon[5], Seok-Gu Kang[6], Hyo Sup Shim[7], Min Hee Hong[2], J. Jean Cui[8], Hye Ryun Kim[2], and Byoung Chul Cho[1,2]

ABSTRACT

Purpose: Although first-line crizotinib treatment leads to clinical benefit in *ROS1*$^{+}$ lung cancer, high prevalence of crizotinib-resistant ROS1-G2032R (ROS1^{G2032R}) mutation and progression in the central nervous system (CNS) represents a therapeutic challenge. Here, we investigated the antitumor activity of repotrectinib, a novel next-generation ROS1/TRK/ALK-tyrosine kinase inhibitor (TKI) in *ROS1*$^{+}$ patient-derived preclinical models.

Experimental Design: Antitumor activity of repotrectinib was evaluated in *ROS1*$^{+}$ patient-derived preclinical models including treatment-naïve and ROS1^{G2032R} models and was further demonstrated in patients enrolled in an on-going phase I/II clinical trial (NCT03093116). Intracranial antitumor activity of repotrectinib was evaluated in a brain-metastasis mouse model.

Results: Repotrectinib potently inhibited *in vitro* and *in vivo* tumor growth and ROS1 downstream signal in treatment-naïve YU1078 compared with clinically available crizotinib, ceritinib, and entrectinib. Despite comparable tumor regression between repotrectinib and lorlatinib in YU1078-derived xenograft model, repotrectinib markedly delayed the onset of tumor recurrence following drug withdrawal. Moreover, repotrectinib induced profound antitumor activity in the CNS with efficient blood–brain barrier penetrating properties. Notably, repotrectinib showed selective and potent *in vitro* and *in vivo* activity against ROS1^{G2032R}. These findings were supported by systemic and intracranial activity of repotrectinib observed in patients enrolled in the on-going clinical trial.

Conclusions: Repotrectinib is a novel next-generation ROS1-TKI with improved potency and selectivity against treatment-naïve and ROS1^{G2032R} with efficient CNS penetration. Our findings suggest that repotrectinib can be effective both as first-line and after progression to prior ROS1-TKI.

Introduction

Chromosomal rearrangements in ros proto-oncogene1 (*ROS1*) gene defines a distinct molecular subset in non–small cell lung cancer (NSCLC; refs. 1–3). The development of ROS1 targeted agents and the approval of crizotinib as a standard first-line therapy has transformed the course of disease for ROS1-driven NSCLC. Although ROS1 tyrosine kinase inhibitors (TKI) markedly improve clinical outcomes, patients inevitably relapse within a few years, and subsequent therapy overcoming acquired resistance remains limited (3, 4). Several major resistance mechanisms to ROS1-TKIs have been identified, including secondary mutations within the ROS1 kinase domain and activation of bypass signaling pathways (1, 5). Approximately 50% to 60% crizotinib-resistant mutations are found within the ROS1 kinase, of which ROS1-G2032R (ROS1^{G2032R}) solvent-front mutation (SFM) is the most common and recalcitrant-resistant mutation. These reports highlight the importance of developing novel ROS1 inhibitors with potent activity against G2032R (1, 6).

The brain is considered a major pharmacologic sanctuary because of the blood–brain barrier (BBB; refs. 7, 8). Indeed, approximately 50% of patients treated with ROS1-TKIs experience disease progression due to central nervous system (CNS) metastases (7, 9). The high incidence of CNS progression and poor prognosis in ROS1-rearranged NSCLC indicates an unmet clinical need for novel ROS1-TKIs with improved efficacy against brain lesions.

Repotrectinib (TPX-0005) is a novel next-generation ROS1/TRK/ALK-TKI specifically designed to overcome refractory SFMs, which commonly emerge in patients with ROS1/NTRK/ALK-rearranged malignancies who have relapsed on currently available TKIs (10). Repotrectinib for TKI-refractory patients is currently under phase I/II clinical trial (NCT03093116).

Existing preclinical studies in ROS1-rearranged NSCLC use a limited number of commercial or genetically engineered cell lines. This fails to fully encompass the genetic complexities observed in patients, leading to discrepancies between preclinical and clinical drug responses. Here, we evaluated the antitumor activity of repotrectinib in

[1]JEUK Institute for Cancer Research, JEUK Co., Ltd., Gumi-City, Kyungbuk, Korea. [2]Division of Medical Oncology, Yonsei Cancer Center, Yonsei University College of Medicine, Seoul, Korea. [3]Severance Biomedical Science Institute, Yonsei University College of Medicine, Seoul, Korea. [4]Department of Hematology-Oncology, Inje University Haeundae Paik Hospital, Busan, Korea. [5]Thoracic Oncology Service, Division of Solid Tumor Oncology, Department of Medicine, Memorial Sloan Kettering Cancer Center, Weill Cornell Medical College, New York, New York. [6]Department of Neurosurgery, Brain Tumor Center, Severance Hospital, Yonsei University College of Medicine, Seoul, Korea. [7]Department of Pathology, Yonsei University College of Medicine, Seoul, Korea. [8]TP Therapeutics, Inc. Department of Chemistry, San Diego, California.

Note: Supplementary data for this article are available at Clinical Cancer Research Online (http://clincancerres.aacrjournals.org/).

M.R. Yun and D.H. Kim contributed equally as co–first authors of this article.

Corresponding Authors: Byoung Chul Cho, Yonsei University College of Medicine, 50 Yonsei-ro, Seodaemun-gu, Seoul 120-752, Republic of Korea. Phone: 822-2228-8126; Fax: 822-393-3652; E-mail: cbc1971@yuhs.ac; Hye Ryun Kim, nobelg@yuhs.ac; and Mi Ran Yun, FORTUNE@yuhs.ac

Clin Cancer Res 2020;26:3287–95

doi: 10.1158/1078-0432.CCR-19-2777

Published OnlineFirst April 8, 2020; DOI: 10.1158/1078-0432.CCR-19-2777

Translational Relevance

We report repotrectinib, a novel next-generation ROS1-TKI as a potent inhibitor against ROS1 and recalcitrant crizotinib-resistant G2032R mutation with efficient activity in the CNS. Repotrectinib demonstrated potent antitumor activity compared with clinically available crizotinib, ceritinib, entrectinib, and lorlatinib in preclinical studies and showed efficient penetration of the BBB with improved survival in brain-metastasis mouse models. These results were confirmed by clinical responses in patients with treatment-naïve and crizotinib-resistant G2032R *ROS1*$^+$ NSCLC. Therefore, repotrectinib could serve as an effective first-line treatment in *ROS1*$^+$ NSCLC, including those with G2032R solvent-front mutation.

ROS1$^+$ NSCLC patient-derived cell lines (PDC) and patient-derived xenograft (PDX) models. Moreover, we examined the intracranial antitumor activity of repotrectinib in a brain-metastasis mouse model developed through intracranial PDC implantation.

Materials and Methods

Patients

All patient samples were obtained from patients with *ROS1* rearrangements before and after treatment with ROS1-TKIs at Yonsei University Severance Hospital (Seoul, Republic of Korea). All patients provided written informed consent. The study protocol was approved by the Institutional Review Board of Severance Hospital (IRB no.: 4-2016-0788). Patients treated with repotrectinib are enrolled in clinical trial NCT-03093116. This study was conducted according to the principles set out in the World Medical Association Declaration of Helsinki and the United States Department of Health and Human Services Belmont Report.

Establishment of PDCs

PDCs were established from malignant effusions of patients with advanced lung adenocarcinoma (11). Briefly, patient pleural effusion samples were centrifuged at 500 × *g* for 10 minutes at 25°C and resuspended in PBS. Cells were separated with Ficoll-Paque PLUS solution, following manufacturer's protocol. The interface containing the mononuclear cells was washed twice in HBSS and plated on collage IV-coated plates in RPMI medium supplemented with 10% FBS. To determine whether PDCs maintained patient characteristics, sanger sequencing and whole-exome sequencing were performed. FACS staining of EpCAM confirmed PDCs with over 99% cancer purity.

The following ROS1-rearranged PDCs were used: YU1078 (CD74-ROS1) and YU1079 (CD74-ROS1 G2032R) (**Table 1**). Sanger-sequencing-identified fusion partners in PDCs were identical to those identified in corresponding patient biopsies.

Establishment of PDXs

ROS1-rearranged PDX model YHIM1047 was established as previously described (**Table 1**; ref. 12).To generate PDC-derived tumor xenograft models, cells (YU1078 and YU1079, 5×10^6 in 100 μL) were implanted subcutaneously into the flanks of 6-week-old female nu/nu mice. Animals were randomly divided ($N = 5$ per group) when tumor volume reached 150 to 200 mm^3. Each group received one of the following treatments: once-daily crizotinib (50 mg/kg, every day), ceritinib (25 mg/kg, every day), entrectinib (30 mg/kg, every day), lorlatinib (30 mg/kg, every day), cabozantinib (30 mg/kg, every day), and twice-daily repotrectinib (15 mg/kg, twice a day). Tumor volumes (0.532 × length × width) were measured with an electronic caliper. Percentage change in tumor volume was calculated as follows: $(V_t - V_0)/V_0 \times 100$. Tumor growth inhibition (TGI) was calculated with two formulas according to Drilon and colleagues (10). All mice were euthanized via CO_2 inhalation at the end of the experiment. Animal procedures were approved by the Institutional Animal Care and Use Committee (IACUC) and Animal Research Committee at Yonsei University College of Medicine.

ROS1 TKIs

Repotrectinib (TP Therapeutics) was kindly provided by the manufacturer and crizotinib, ceritinib, entrectinib, lorlatinib, and cabozantinib were purchased from Selleckchem.

Cell proliferation assay

About 2,500 to 3,000 cells were seeded in 96-well plates in growth media and incubated overnight at 37°C before adding serially diluted crizotinib, ceritinib, lorlatinib, cabozantinib, repotrectinib, and appropriate controls. After treating the drugs, cells were incubated at 37°C for 72 hours before performing CellTiter Glo (Promega) following the manufacturer's protocol. Dose–response curves and IC_{50} values were calculated using GraphPad Prism.

Colony-forming assays were performed by seeding the cells in six-well plates in growth media with appropriate drug-containing media replaced every 3 days. Plates were fixed in 4% PFA and stained in crystal violet for 1 hour after 14 days of drug treatment.

Immunoblotting

Immunoblots were performed to determine relative phosphorylation of kinases and total protein levels of interest. Protein samples were separated by SPS-PAGE and transferred to nitrocellulose membrane for immunoblotting using the corresponding antibodies. P-ROS1 (T2274), ROS1, p-ERK (T202/Y204), ERK, p-AKT (S473), AKT, p-STAT3 (T705), STAT3, and Ki67 were all purchased from Cell Signaling Technologies. β-Actin was purchased from Sigma.

Intracranial tumor model

Intracranial tumor models were generated through implanting YU1078-luc human NSCLC PDC into brains of female BALB/c nude mice. After anesthetization, mice were immobilized with a stereotactic apparatus for incision of the skull's right hemisphere. A 0.5 mm burr hole was drilled through the right frontal lobe to implant a guide screw. Next, 5×10^5 cancer cells (diluted in 5 μL PBS) were stereotactically injected for 5 minutes into the right frontal lobe via the guided screw and the incision was closed with surgical glue. At 13-day post-implantation, when photon flux measured through IVIS reached 1×10^6 photons/second, mice were treated with a daily oral dose of repotrectinib (15 mg/kg, twice a day), entrectinib (30 mg/kg, every day), lorlatinib (30 mg/kg, every day), and vehicle. Brain metastatic-tumor growth was measured using an IVIS Spectrum Xenogen (Caliper Life Sciences).

Immunohistochemistry

IHC was performed on 4-μm-thick formalin-fixed, paraffin-embedded (FFPE) tissue sections. Slides were baked, deparaffinized in xylene, passed through graded alcohols, and then antigen retrieved with 1 mmol/L EDTA, pH 8.0 at 125°C for 30 seconds. Slides were pretreated with Peroxidase Block (Dako USA) for 5 minutes, and then washed in 50 mmol/L Tris-Cl, pH 7.4. Slides were blocked using

Published OnlineFirst April 8, 2020; DOI: 10.1158/1078-0432.CCR-19-2777

Table 1. PDCs, PDXs, and tumor biopsies from patients with *ROS1*-rearranged NSCLC.

Patient	Type	Model ID	Fusion partner	Biopsy site	ROS1 mutation	Targeted therapy preceding biopsy	Best RECIST response	Treatment duration (months)
Patient #1-1	PDC	YU1078	CD74-ROS1	Pleural effusion	WT	Naïve	—	—
Patient #1-2	PDC	YU1079	CD74-ROS1	Pleural effusion	G2032R	Crizotinib	PR	10
Patient #2	PDX	YHIM1047	CD74-ROS1	Lung	G2032R	Entrectinib	PR	7
Patient A	Patient biopsy	—	CD74-ROS1	Lung	WT	Repotrectinib	PR	10
Patient B	Patient biopsy	—	SLC34A2-ROS1	Lung	WT	Repotrectinib	PR	10

Abbreviations: PR, partial response; WT, wild-type.

normal goat serum (Dako USA), and subsequently incubated with anti-phosphSTAT3 mAb (Tyr705, D3A2, 1:100; CST)/anti-Ki67 antibody (D2H10; 1:100) for 1 hour. Slides were then washed in 50 mmol/L Tris-Cl, pH7.4 and treated with Signalstain boost IHC detection reagent [horseradish peroxidase (HRP), rabbit, #8114; CST] for 30 minutes. After further washing, immunoperoxidase staining was developed using a 3,3′diaminobenzidine (DAB) chromogen (Dako) for 5 minutes. Slides were counterstained with hematoxylin, dehydrated in graded alcohol and xylene, mounted, and coverslipped.

Targeted sequencing

Comprehensive genomic profiling was performed in repeat biopsies in 2 patients who progressed after repotrectinib. FFPE slides were subjected to Illumina HiSeq based targeted sequencing capturing 171 cancer-related genes. Resultant reads were mapped to the human genome reference (hg19) using Burrows-Wheeler Alignment (BWA) followed by analysis using Genome Analysis ToolKit. Somatic mutations were called using MuTect2 and annotated with Oncotator. FoundationOne CDx (Foundation Medicine) was used to confirm the identified genomic alterations. A whole-genome shotgun library was constructed from 50 to 1,000 ng of extracted DNA and hybrid capture-selected libraries were sequenced at >500× median coverage using the Illumina HiSeq platform. All classes of cancer-related genomic alterations (e.g., base substitutions, indels, rearrangements, and copy-number alterations) were assayed.

Statistical analysis

Statistical analyses were performed in SPSS version 21 and GraphPad Prism 5. All data are expressed as means ± SD or ±SE for three or more independent replications. Between-group differences were evaluated using Student *t* test, Mann–Whitney test, Kruskal–Wallis with Dunn *post hoc* test, or ANOVA with Tukey *post hoc* test, as appropriate. Significance was set at $P < 0.05$.

Results

Repotrectinib potently inhibits *in vitro* and *in vivo* tumor growth in treatment-naïve ROS1-rearranged models

In this study, we established three patient-derived preclinical models including one treatment-naive and two ROS1-TKI–resistant models from patients with *ROS1*$^+$ NSCLC (**Table 1**). We examined the activities of clinically available ROS1-TKIs including crizotinib, ceritinib, entrectinib, lorlatinib, and repotrectinib in treatment-naive PDC YU1078 cells generated from a patient with ROS1-TKI–naïve NSCLC with *CD74–ROS1* (35 years/female). Entrectinib (IC_{50}, 0.052 μmol/L), lorlatinib (IC_{50}, 0.009 μmol/L), and repotrectinib (IC_{50}, 0.021 μmol/L) exhibited potent growth inhibition in YU1078 cells compared with crizotinib (IC_{50}, 0.156 μmol/L) and ceritinib (IC_{50}, 0.412 μmol/L; **Fig. 1A**). Colony formation was significantly reduced with lorlatinib and repotrectinib treatment compared with other TKIs (**Fig. 1B**) and was accompanied by markedly suppressed ROS1 and ERK phosphorylation levels (**Fig. 1C**).

Consistent with the *in vitro* findings, lorlatinib and repotrectinib displayed pronounced tumor regression in subcutaneous YU1078 xenograft model with 189.2% TGI. Crizotinib and entrectinib resulted in 150.7% and 124.9% TGI, respectively, whereas ceritinib displayed 64.7% TGI (**Fig. 1D**). Although tumor regression was comparable between lorlatinib and repotrectinib, repotrectinib produced the strongest antitumor effect, which was most apparent after drug withdrawal. After drug withdrawal at 21 days, tumors in three of four repotrectinib-treated mice were persistently suppressed for over 80 days. One mouse exhibited slow regrowth after 60 days post-drug withdrawal. However, tumors in two of four lorlatinib-treated mice abruptly regrew 10 days after drug withdrawal (**Fig. 1E**). To determine whether repotrectinib is an effective subsequent treatment option after failure to prior ROS1-TKI, we administrated repotrectinib to tumor progressed on ceritinib. Subsequent repotrectinib treatment prominently suppressed tumor growth where of note, upfront repotrectinib completely induced tumor regression (**Fig. 1F**). Collectively, upfront and subsequent repotrectinib treatment demonstrated potent TGI based on *in vitro* and *in vivo ROS1*$^+$ preclinical models.

Repotrectinib demonstrates efficient antitumor activity in an intracranial tumor model with a high BBB penetration profile

Lorlatinib and entrectinib have been reported to penetrate the BBB and regress brain metastasis (13–15). We investigated the ability of repotrectinib to penetrate BBB using an intracranial tumor model of luciferase-transduced YU1078 cells (YU1078-luc). Compared with vehicle and entrectinib, repotrectinib treatment significantly reduced tumor load (as measured using photon flux) in the brain without body weight loss (**Fig. 2A** and **B**). In addition, all repotrectinib-treated mice survived for up to 110 days, whereas median survival of vehicle- and entrectinib-treated mice was 49 and 57 days, respectively (**Fig. 2C**). Lorlatinib showed comparable reduction of tumor load to that of repotrectinib (**Fig. 2A** and **B**). IHC further revealed that repotrectinib treatment completely suppressed viable brain tumors, with pronounced reduction in Ki67-positive and TUNEL-positive cells compared with vehicle and entrectinib treatment (**Fig. 2D**).

Clinical activity of repotrectinib in ROS1-TKI–naïve and ceritinib-resistant patients

Clinical potency of repotrectinib was demonstrated in a TKI-naïve *ROS1*$^+$ patient treated with repotrectinib. A 69-year-old female *CD74-ROS1*–rearranged patient was presented with liver and multiple brain

Published OnlineFirst April 8, 2020; DOI: 10.1158/1078-0432.CCR-19-2777

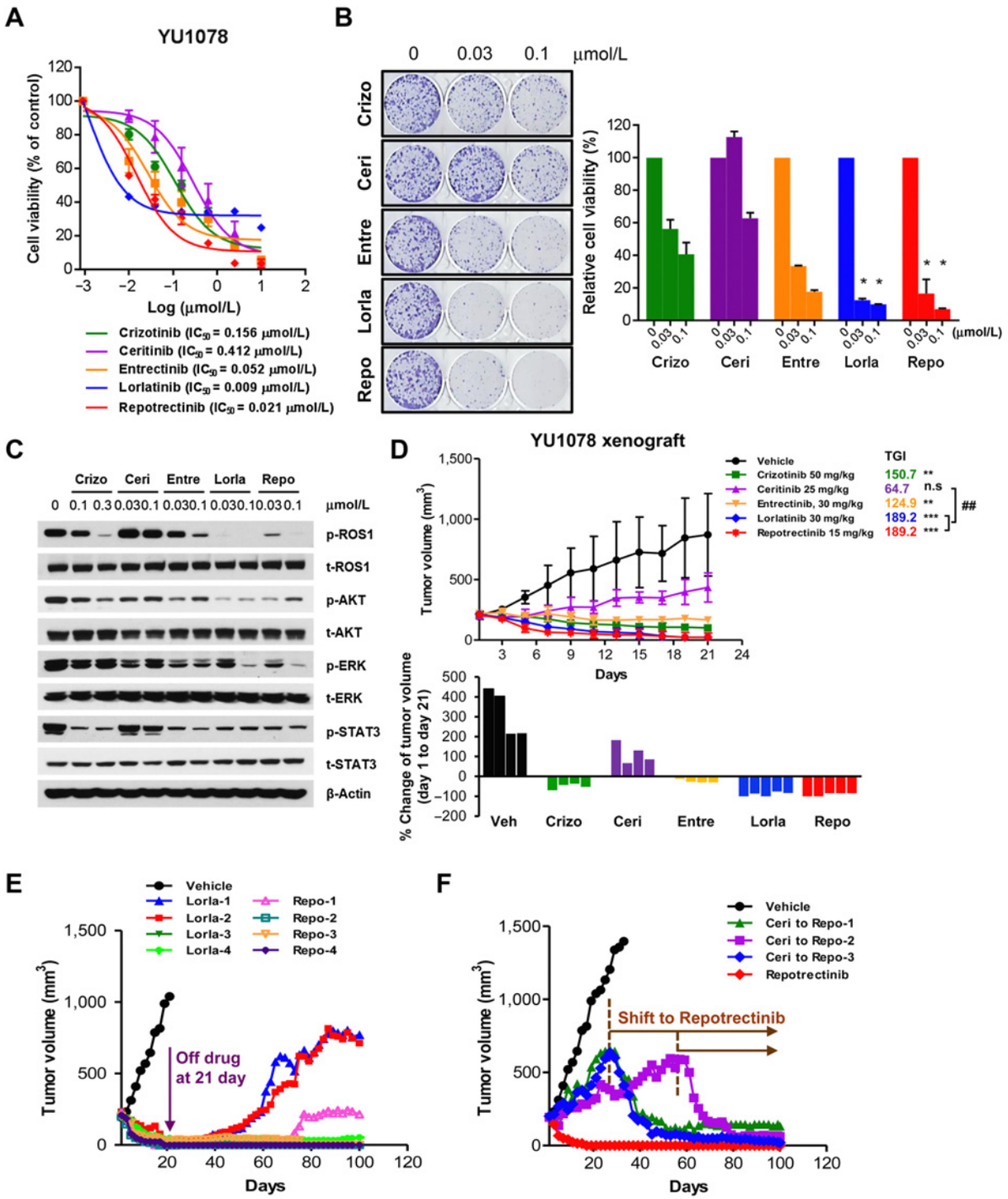

Figure 1.

In vitro and *in vivo* inhibitory activity of repotrectinib in treatment-naïve *ROS1*$^{+}$ patient-derived preclinical models. **A,** Cell viability assay of CD74-ROS1 YU1078 treated with ROS1-TKIs for 72 hours. **B,** Colony formation assays involved treatment for 14 days with the indicated dose of ROS1-TKIs; corresponding colony quantification on the right (ANOVA with Tukey *post hoc* test: *, $P < 0.05$ vs. crizotinib). **C,** Immunoblots of YU1078 after treatment with indicated crizotinib, ceritinib, entrectinib, lorlatinib, and repotrectinib doses for 6 hours. **D,** Tumor growth of subcutaneous YU1078 xenograft in response to TKI treatment (Kruskal–Wallis with Dunn *post hoc* test: n.s., $P > 0.05$; **, $P < 0.01$; ***, $P < 0.001$ vs. vehicle; $^{\#\#}$, $P < 0.01$ vs. ceritinib, $N = 4$). Corresponding waterfall plot below represents individual mouse response. **E,** Tumor growth in individual mice after withdrawal of lorlatinib and repotrectinib at 21 days and (**F**) treatment shift to repotrectinib in ceritinib-treated tumors from (**D**). Data are mean ± SD or ± SE.

Published OnlineFirst April 8, 2020; DOI: 10.1158/1078-0432.CCR-19-2777

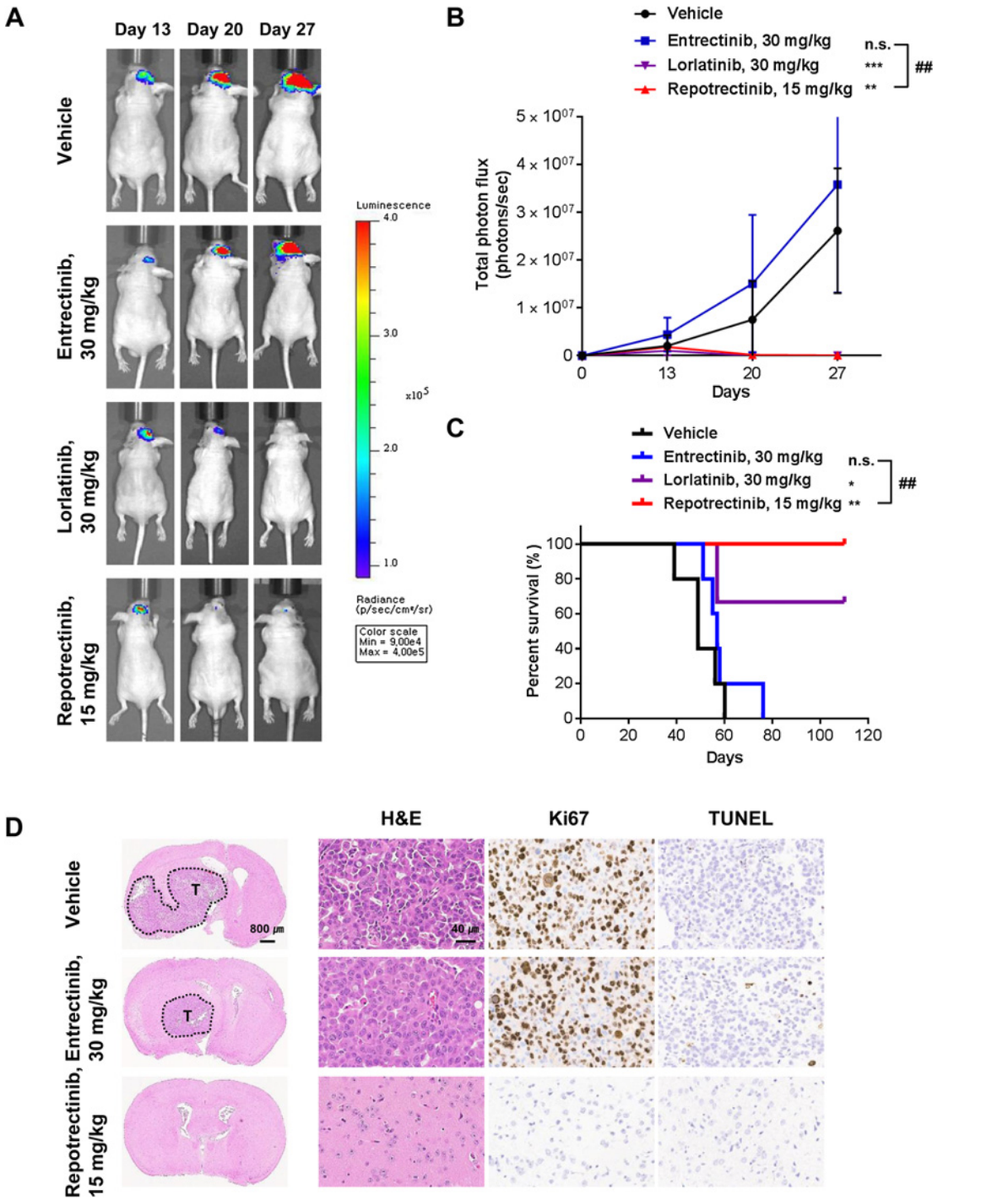

Figure 2.

Antitumor efficacy of repotrectinib in *ROS1*$^{+}$ PDC-driven intracranial tumor models. **A,** Representative IVIS image of intracranial YU1078-luc cells treated with entrectinib once daily, lorlatinib once daily, and repotrectinib twice daily. Mice were orally dosed 13 days after intracranial injection. **B,** Average photon count (photons/s) of intracranial metastasis over 27 days. Data are mean ± SD. Significance between groups observed at 27 days (Mann–Whitney test: n.s., $P > 0.05$; **, $P < 0.01$; ***, $P < 0.001$ vs. vehicle; $^{\#\#}$, $P < 0.01$ vs. entrectinib, $N = 5$; lorlatinib, $N = 3$). **C,** Kaplan–Meier survival curve of YU1078-luc injected mice (log-rank test: n.s., $P > 0.05$; **, $P < 0.01$ vs. vehicle; $^{\#\#}$, $P < 0.01$ vs. entrectinib, $N = 5$; lorlatinib, $n = 3$). **D,** Representative hematoxylin and eosin (H&E), Ki67, and TUNEL staining of brain sections following entrectinib and repotrectinib treatments.

Published OnlineFirst April 8, 2020; DOI: 10.1158/1078-0432.CCR-19-2777

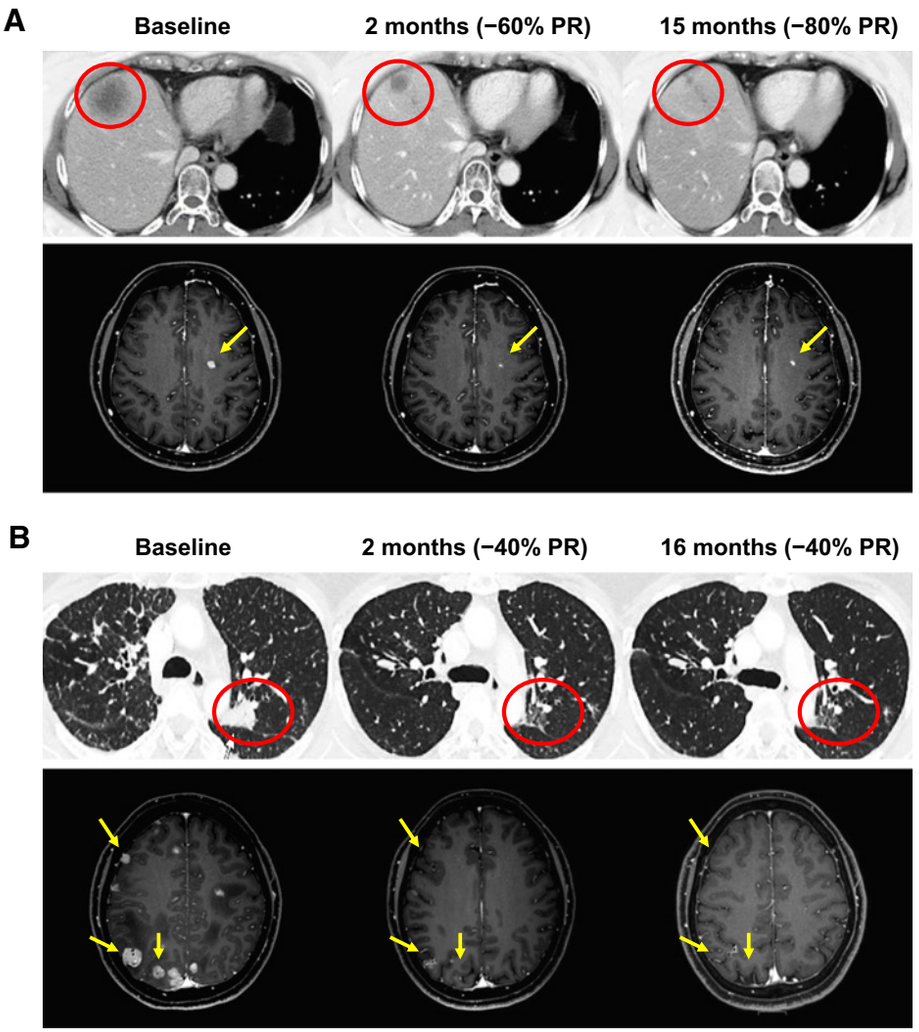

Figure 3.
Favorable response to repotrectinib in ROS1-TKI treatment-naïve and ceritinib-resistant patients. **A,** Confirmed partial response in a *CD74-ROS1* NSCLC patient based on RECIST1.1 of hepatic and brain metastasis, after treatment with 40 mg repotrectinib once daily, at 2 months and 16 months. **B,** Confirmed partial response of lung and brain metastasis in a patient with *CD74-ROS1* NSCLC who progressed on ceritinib, after treatment with 40 mg (increased to 240 mg) repotrectinib once daily. Red circles and yellow arrows indicate areas of metastatic tumor disease.

metastases. After receiving 40 mg repotrectinib once daily on the phase I repotrectinib trial, the patient achieved confirmed PR (−80%) based on RECIST1.1, currently ongoing at 20 months (**Fig. 3A**). The phase I repotrectinib trial also included a *ROS1*$^{+}$ lung cancer patient who had recurred under ceritinib. Pre-repotrectinib brain imaging revealed multiple asymptomatic brain metastases. This patient tolerated repotrectinib treatment (40–240 mg, every day) and achieved confirmed RECIST1.1-based PR (−40%) that is ongoing at 16 months (**Fig. 3B**). As a clinical proof of concept, the potent intracranial activity of repotrectinib has been observed in a TKI-naïve patient and a patient who had progressed on prior TKI enrolled in an ongoing phase I/II clinical trial. Multiple metastatic brain lesions disappeared after 2-month treatment and were maintained over 15 months in each patient.

Repotrectinib overcomes crizotinib-resistant ROS1^{G2032R}

We identified the ROS1^{G2032R} mutation in YU1079, which was serially established in the same patient as YU1078 but after progressing on crizotinib treatment. On the basis of recent studies examining lorlatinib and cabozantinib in Ba/F3 cells engineered with CD74–ROS1^{G2032R} (10, 13), we investigated these TKIs in our YU1079 with CD74-ROS1^{G2032R}. Cabozantinib (IC_{50}, 0.111 μmol/L) and repotrectinib (IC_{50}, 0.097 μmol/L) effectively inhibited YU1079 ROS1^{G2032R} growth, concomitant with marked reduction in ROS1 and downstream signal phosphorylation (**Fig. 4A–C**). However, lorlatinib (IC_{50}, 1.509 μmol/L) was relatively ineffective in inhibiting YU1079 ROS1^{G2032R} growth, possibly due to a weak inhibitory effect on phospho-ROS1, ERK, and STAT3, along with persistent phospho-AKT (**Fig. 4C**).

The *in vivo* efficacy of these TKIs was further evaluated in YU1079 ROS1^{G2032R} PDX model. Consistent with the *in vitro* assays, cabozantinib and repotrectinib significantly led to 102.1% and 90.9% TGI, respectively, compared with 22.7% TGI for lorlatinib (**Fig. 4D**). Considering severe treatment-related toxicities observed in patients receiving cabozantinib (1, 16, 17), we focused on comparing repotrectinib with clinically available entrectinib in the PDX model YHIM1047 ROS1^{G2032R}, established from a *CD74-ROS1* patient with NSCLC who progressed on entrectinib. As expected from the patient's clinical response, entrectinib failed to inhibit tumor growth whereas repotrectinib treatment induced 142.8% TGI (**Fig. 4E**). IHC revealed marked reduction of phosphorylated STAT3 and Ki67 in repotrectinib-treated YHIM1047 ROS1^{G2032R} tumors compared with entrectinib and vehicle (**Fig. 4F**).

Published OnlineFirst April 8, 2020; DOI: 10.1158/1078-0432.CCR-19-2777

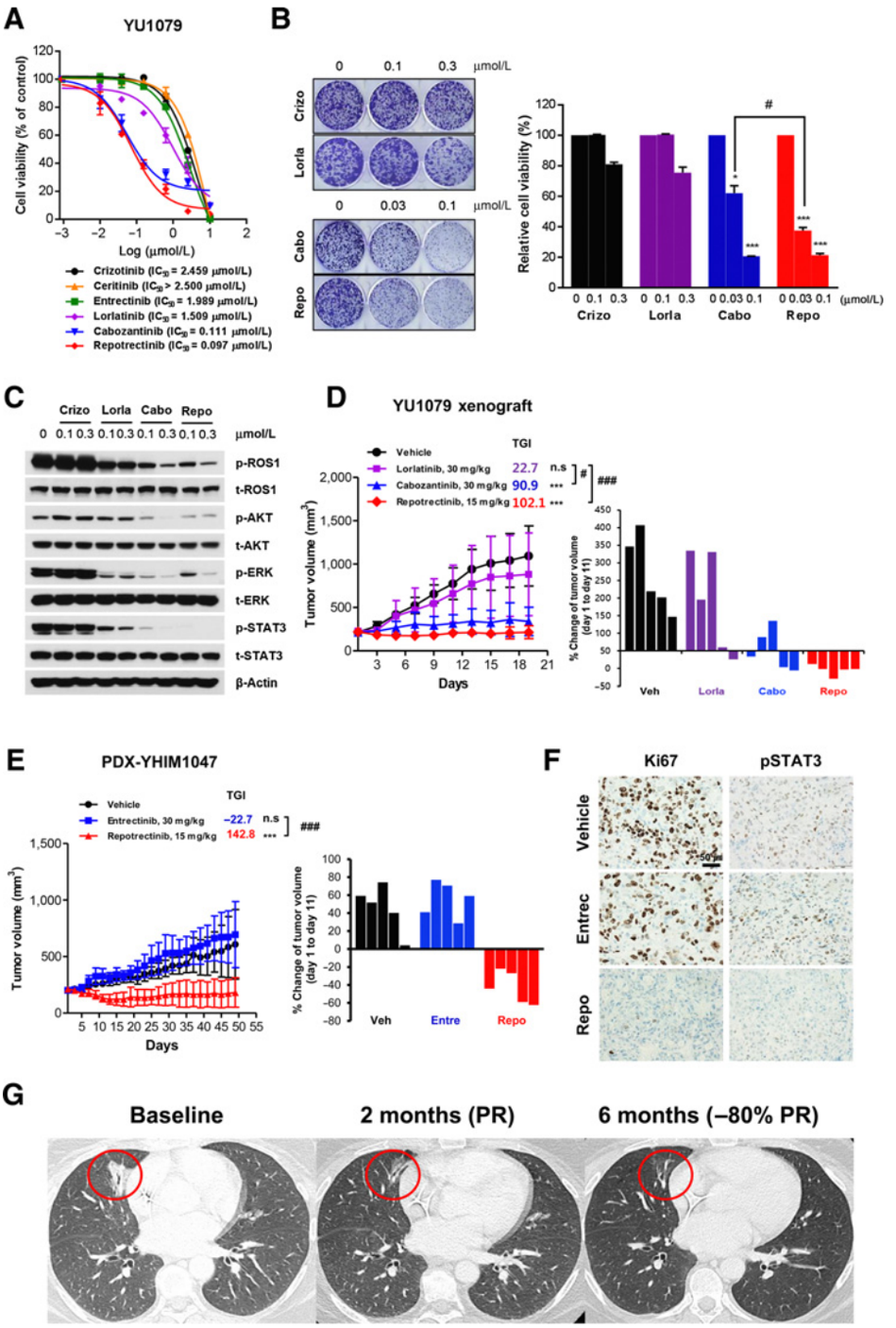

Figure 4.

Antitumor efficacy of repotrectinib against crizotinib-resistant ROS1 SFM G2032R. **A,** Cell viability assay of CD74-ROS1^{G2032R}–mutant YU1079 treated with ROS1-TKIs for 72 hours. **B,** Colony formation assays involved treatment for 14 days with the indicated dose of ROS1-TKIs; corresponding colony quantification on the right (ANOVA with Tukey *post hoc* test: *, $P < 0.05$; ***, $P < 0.001$ vs. crizotinib; $^{\#}$, $P < 0.05$ vs. cabozantinib). **C,** Immunoblots of YU1079 after 6 hours treatment with indicated crizotinib, lorlatinib, cabozantinib, and repotrectinib doses. **D,** Tumor growth of YU1079 xenograft in response to TKI treatment (Kruskal–Wallis with Dunn *post hoc* test: n.s., $P > 0.05$; ***, $P < 0.001$ vs. vehicle; $^{\#}$, $P < 0.05$; $^{\#\#\#}$, $P < 0.001$ vs. lorlatinib, $N = 5$). Corresponding waterfall plot on the right represents individual mouse response. **E,** Tumor growth of PDX model YHIM1047 harboring CD74-ROS1^{G2032R} mutation ($N = 5$) treated with entrectinib and repotrectinib. Corresponding waterfall plot on the right represents individual mouse response. **F,** Representative Ki67 and pSTAT3 staining of tumor sections following entrectinib and repotrectinib treatments. Data are mean ± SD or ± SE. **G,** Confirmed partial response in a CD74-ROS1^{G2032R}–mutant NSCLC patient who progressed on crizotinib based on RECIST1.1, after treatment with 160 mg repotrectinib twice daily, at 2 and 6 months. Red circles indicate areas of metastatic disease.

The clinical activity of repotrectinib against ROS1 SFM was seen in a 49-year-old female *ROS1*-rearranged patient who progressed after 44 months of crizotinib treatment with an identified CD74-ROS1 G2032R mutation. The patient received 160 mg twice a day repotrectinib which induced a confirmed PR (−80%) based on RECIST1.1 currently ongoing at 6 months (**Fig. 4G**). Taken together, these results suggest that repotrectinib is a promising therapeutic strategy for *ROS1*-rearranged NSCLC harboring ROS1^{G2032R}.

Genetic alterations in *ROS1*-rearranged patients who progressed on repotrectinib

Finally, we investigated genetic mutation status in biopsies of 2 patients who progressed on repotrectinib in clinical trial using targeted sequencing. Patient A, a 46-year-old male with a 20 pack-year smoking history, was diagnosed with adenocarcinoma. The patient underwent a first biopsy before treatment, followed by a second biopsy after progression on repotrectinib treatment for about 10 months (**Table 1**).

Published OnlineFirst April 8, 2020; DOI: 10.1158/1078-0432.CCR-19-2777

A variant of the ROS1 translocation, CD74-ROS1 fusion, was detected by targeted sequencing. Mutations in the ROS1 kinase domain were not detected. Post-repotrectinib tumor biopsy had mutations in CCND3 (E253Q), TP53 (H178Q&H179Y), and SMAD4 (E538*), which were absent in the corresponding baseline biopsy (Supplementary Table S1). These mutations occurred at different variant allele frequencies (VAF), 7%, 53%, and 47%, respectively. Patient B was a 38-year-old female with adenocarcinoma with a 10 pack-year smoking history. The patient was biopsied following progression on repotrectinib after 10 months of treatment (**Table 1**). ROS1 fusion partner was identified as SLC34A2. We identified CEBPA (196_197insHP, VAF 41%), RB1 (H555R, VAF 45%), ERBB2 (R143Q, VAF 51%), and TP53 (E171G, VAF 9%) mutations in the post-repotrectinib tumor biopsy. We were unable to demonstrate the absence of these mutations in the baseline biopsy due to lack of available tumor tissue. Altogether, these findings suggest the possibility of non-ROS1 dominant mechanism as acquired resistance to repotrectinib. Further studies are necessary to investigate the functional role of these mutations to elucidate acquired resistance mechanism to repotrectinib.

Discussion

In this study, we demonstrated that repotrectinib is a potent next-generation TKI against ROS1 and ROS1^{G2032R} mutation with remarkable activity in the CNS. Our findings highlight the potential of repotrectinib as a first-line therapy in *ROS1*$^{+}$ NSCLC as well as those with G2032R.

Crizotinib is the FDA-approved standard care in *ROS1*-rearranged NSCLC with entrectinib emerging as a promising ROS1-TKI recently approved by the FDA. Ceritinib and lorlatinib have both previously showed clinical activity in treatment-naïve *ROS1*$^{+}$ NSCLC (8, 18). In particular, lorlatinib is the only recommended TKI after progression to crizotinib under National Comprehensive Cancer Network (NCCN) guidelines (19). To our knowledge, repotrectinib exhibited the most potent *in vitro* and *in vivo* activity compared with other ROS1-TKIs in treatment-naïve YU1078 model (**Fig. 1A–D**). Despite comparable activity between repotrectinib and lorlatinib, repotrectinib was able to persistently and strongly suppress tumor recurrence in YU1078-derived xenograft model for more than 80 days even after drug withdrawal (**Fig. 1E**). Consistent with previous reports (10), our findings suggest that repotrectinib is a potent ROS1-TKI in the first-line setting.

CNS metastases remain a major cause of morbidity and mortality in ROS1-driven NSCLC. Recent reports highlighted that 36% of *ROS1*$^{+}$ patients experience CNS metastasis at baseline or 50% after crizotinib treatment similar to *ALK*+ NSCLC (9). The low brain-to-plasma ratio of crizotinib suggests that frequent CNS metastasis during crizotinib treatment may be due to poor BBB penetration and brain exposure (6). For the first time, we demonstrated superior CNS penetration of repotrectinib compared with entrectinib in YU1078-luc intracranial tumor model with significant reduction of metastatic brain lesion and extensive mouse survival over 100 days (**Fig. 2**). This was clinically supported by two *CD74-ROS1* NSCLC patient response data where repotrectinib rapidly regressed tumor and the metastatic brain lesion (**Fig. 3**). Therefore, upfront repotrectinib therapy could effectively reduce dismal prognosis due to CNS progression, which might overcome current limitations of first-line crizotinib.

Acquired resistance to targeted therapy is a major obstacle for achieving durable response in oncogene-driven NSCLC. Approximately 50% to 60% of acquired resistance to crizotinib is caused by on-target mutations, of which G2032R is the most recalcitrant and commonly observed mutation in *ROS1*$^{+}$ patients. Ceritinib, entrectinib, and lorlatinib did not show robust activity against G2032R, as reported previously (10, 13). Cabozantinib exhibited comparable activity to repotrectinib but toxicity observed in clinical trials should be managed further (16). Recently, a novel ROS1/NTRK inhibitor DS-6051b was reported to have activity against G2032R in preclinical models but requires validation in the clinical setting (20). Consistent with previous reports demonstrating the activity of repotrectinib in BaF3 CD74–ROS1^{G2032R} cell line and xenograft models (10), we demonstrated prominent antitumor activity of repotrectinib in crizotinib-refractory YU1079 ROS1^{G2032R} and entrectinib-refractory YHIM1047 ROS1^{G2032R}. This was supported by pronounced tumor regression in patient with CD74-ROS1 G2032R NSCLC (**Fig. 4**). Recently, preliminary results of TRIDENT1 trial reported meaningful clinical activity and favorable safety profiles of repotrectinib (21, 22). The confirmed objective response rate (ORR) was 91% in 11 patients with TKI-naïve *ROS1*$^{+}$ NSCLC and 39% in 18 TKI-pretreated patients after repotrectinib. ROS1^{G2032R} patients demonstrated ORR 43% (n = 3/7). Most adverse events were manageable and grade 1 to 2. Collectively, repotrectinib is an effective therapy against *ROS1*$^{+}$ NSCLC patients who are TKI-naïve or TKI-refractory harboring G2032R.

Upfront next-generation TKI therapy prolonged survival outcome in patients with EGFR-mut and ALK-fusion NSCLC and have been approved as standard care in these patients (23, 24). Moreover, a recent study presented that sequential ALK-TKI treatment fosters development of diverse compound mutations, highly refractory to all available ALK-inhibitors (25). These data implicate that upfront use of repotrectinib could be able to prevent or delay the emergence of G2032R and subsequent compound mutations, potentially improving clinical outcomes. In line with the idea, G2032R or ROS1 compound mutation was not observed in 2 patients who progressed on first-line repotrectinib in our study (Supplementary Table S1). Therefore, optimal first-line therapy could be derived from repotrectinib-based combinations to prevent both ROS1-dependent and -independent resistance. Potent overall and intracranial activity, G2032R specificity, and favorable safety profiles suggest repotrectinib as a promising first-line TKI.

In conclusion, we demonstrated that repotrectinib is a novel, highly potent, BBB-penetrant next-generation ROS1/TRK/ALK-TKI. Our findings provide evidence for repotrectinib as an effective first-line treatment in *ROS1*$^{+}$ NSCLC and after progression to prior ROS1-TKI.

Disclosure of Potential Conflicts of Interest

A. Drilon is an employee/paid consultant for Ignyta/Genentech/Roche, LOXO/Bayer/Lilly, Takeda/Ariad/Millenium, TP Therapeutics, AstraZeneca, Pfizer, Blueprint, Helsinn, Beigene, BergenBio, Hengrui, Exelixis, Tyra, Verastem/14ner, MOREHealth, and Abbvie, and reports receiving other remuneration from GlaxoSmithKline, Teva, Taiho, PharmaMar, Foundation Medicine, Wolters Kluwer, and Merck/Puma/Merus/Boehringer Ingelheim. B. Chul Cho is an employee/paid consultant for Novartis, AstraZeneca, Boehringer-Ingelheim, Roche, Bristol-Myers Squibb, Ono, Yuhan, Pfizer, Eli Lilly, Janssen, Takeda, and MSD, and reports receiving commercial research grants from Novartis, Bayer, AstraZeneca, MOGAM Institute, Dong-A ST, Champions Oncology, Janssen, Yuhan, Ono, Dizal Pharma, and MSD, and reports receiving speakers bureau honoraria from Novartis, Bayer, AstraZeneca, MOGAM Institute, Dong-A ST, Champions Oncology, Janssen, Yuhan, Ono, Dizal Pharma, and MSD, and holds ownership interest (including patents) in TheraCanVac Inc., Gencurix Inc., and Bridgebio Therapeutics. No potential conflicts of interest were disclosed by the other authors.

Authors' Contributions

Conception and design: M.R. Yun, D.H. Kim, Y.W. Lee, J.J. Cui, H.R. Kim
Development of methodology: D.H. Kim, S.-G. Kang
Acquisition of data (provided animals, acquired and managed patients, provided facilities, etc.): D.H. Kim, S.-Y. Kim, H.-S. Joo, H.M. Choi, A. Drilon, H.S. Shim, J.J. Cui, H.R. Kim
Analysis and interpretation of data (e.g., statistical analysis, biostatistics, computational analysis): D.H. Kim, S.G. Heo, A.J. Schoenfeld, A. Drilon, H.S. Shim, J.J. Cui, H.R. Kim
Writing, review, and/or revision of the manuscript: D.H. Kim, A.J. Schoenfeld, A. Drilon, H.S. Shim, M.H. Hong, J.J. Cui, H.R. Kim
Administrative, technical, or material support (i.e., reporting or organizing data, constructing databases): C.W. Park, H.N. Kang, S.S. Lee, M.H. Hong
Study supervision: M.R. Yun, B.C. Cho

Acknowledgments

We thank all the patients who participated in this study. This research was supported by Basic Science Research Program through the National Research Foundation of Korea (NRF) funded by the Ministry of Science, ICT & Future Planning (2016R1A2B3016282, to B.C. Cho) and NRF grant funded by the Korean government (NRF-2018R1D1A1B07050233, to M.R. Yun).

The costs of publication of this article were defrayed in part by the payment of page charges. This article must therefore be hereby marked *advertisement* in accordance with 18 U.S.C. Section 1734 solely to indicate this fact.

Received August 22, 2019; revised January 15, 2020; accepted February 17, 2020; published first April 8, 2020.

References

1. Lin JJ, Shaw AT. Recent advances in targeting ROS1 in lung cancer. J Thorac Oncol 2017;12:1611–25.
2. Kim HR, Lim SM, Kim HJ, Hwang SK, Park JK, Shin E, et al. The frequency and impact of ROS1 rearrangement on clinical outcomes in never smokers with lung adenocarcinoma. Ann Oncol 2013;24:2364–70.
3. Song A, Kim TM, Kim DW, Kim S, Keam B, Lee SH, et al. Molecular changes associated with acquired resistance to crizotinib in ROS1-rearranged non-small cell lung cancer. Clin Cancer Res 2015;21:2379–87.
4. Schram AM, Chang MT, Jonsson P, Drilon A. Fusions in solid tumours: diagnostic strategies, targeted therapy, and acquired resistance. Nat Rev Clin Oncol 2017;14:735–48.
5. Rotow J, Bivona TG. Understanding and targeting resistance mechanisms in NSCLC. Nat Rev Cancer 2017;17:637–58.
6. Gainor JF, Tseng D, Yoda S, Dagogo-Jack I, Friboulet L, Lin JJ, et al. Patterns of metastatic spread and mechanisms of resistance to crizotinib in ROS1-positive non-small-cell lung cancer. JCO Precis Oncol 2017;2017:1–13.
7. Park S, Ahn BC, Lim SW, Sun JM, Kim HR, Hong MH, et al. Characteristics and outcome of ROS1-positive non-small cell lung cancer patients in routine clinical practice. J Thorac Oncol 2018;13:1373–82.
8. Lim SM, Kim HR, Lee JS, Lee KH, Lee YG, Min YJ, et al. Open-label, multicenter, phase II study of ceritinib in patients with non-small-cell lung cancer harboring ROS1 rearrangement. J Clin Oncol 2017;35:2613–8.
9. Patil T, Smith DE, Bunn PA, Aisner DL, Le AT, Hancock M, et al. The incidence of brain metastases in stage IV ROS1-rearranged non–small cell lung cancer and rate of central nervous system progression on crizotinib. J Thorac Oncol 2018;13:1717–26.
10. Drilon A, Ou SI, Cho BC, Kim DW, Lee J, Lin JJ, et al. Repotrectinib (TPX-0005) is a next-generation ROS1/TRK/ALK inhibitor that potently inhibits ROS1/TRK/ALK solvent- front mutations. Cancer Discov 2018;8:1227–36.
11. Kim S-Y, Lee JY, Kim DH, Joo HS, Yun MR, Jung D, et al. Patient-derived cells to guide targeted therapy for advanced lung adenocarcinoma. Sci Rep 2019;9:19909.
12. Kang HN, Choi JW, Shim HS, Kim J, Kim DJ, Lee CY, et al. Establishment of a platform of non-small-cell lung cancer patient-derived xenografts with clinical and genomic annotation. Lung Cancer 2018;124:168–78.
13. Zou HY, Li Q, Engstrom LD, West M, Appleman V, Wong KA, et al. PF-06463922 is a potent and selective next-generation ROS1/ALK inhibitor capable of blocking crizotinib-resistant ROS1 mutations. Proc Natl Acad Sci U S A 2015;112:3493–8.
14. Solomon BJ, Besse B, Bauer TM, Felip E, Soo RA, Camidge DR, et al. Lorlatinib in patients with ALK-positive non-small-cell lung cancer: results from a global phase 2 study. Lancet Oncol 2018;19:1654–67.
15. Ardini E, Menichincheri M, Banfi P, Bosotti R, De Ponti C, Pulci R, et al. Entrectinib, a pan-TRK, ROS1, and ALK inhibitor with activity in multiple molecularly defined cancer indications. Mol Cancer Ther 2016;15:628–39.
16. Drilon A, Rekhtman N, Arcila M, Wang L, Ni A, Albano M, et al. Cabozantinib in patients with advanced RET-rearranged non-small-cell lung cancer: an open-label, single-centre, phase 2, single-arm trial. Lancet Oncol 2016;17:1653–60.
17. Guisier F, Piton N, Salaun M, Thiberville L. ROS1-rearranged NSCLC with secondary resistance mutation: case report and current perspectives. Clin Lung Cancer 2019;20:e593–e6.
18. Shaw AT, Felip E, Bauer TM, Besse B, Navarro A, Postel-Vinay S, et al. Lorlatinib in non-small-cell lung cancer with ALK or ROS1 rearrangement: an international, multicentre, open-label, single-arm first-in-man phase 1 trial. Lancet Oncol 2017;18:1590–9.
19. Ettinger DS, Wood DE, Aggarwal C, Aisner DL, Akerley W, Bauman J, et al. Non-small cell lung cancer, version 2.2020, NCCN Clinical Practice Guidelines in Oncology; 2020. Available from: https://www.nccn.org/professionals/physician_gls/pdf/nscl.pdf.
20. Katayama R, Gong B, Togashi N, Miyamoto M, Kiga M, Iwasaki S, et al. The new-generation selective ROS1/NTRK inhibitor DS-6051b overcomes crizotinib resistant ROS1-G2032R mutation in preclinical models. Nat Commun 2019;10:3604.
21. Cho BC, Drilon AE, Doebele RC, Kim D-W, Lin JJ, Lee J, et al. Safety and preliminary clinical activity of repotrectinib in patients with advanced ROS1 fusion-positive non-small cell lung cancer (TRIDENT-1 study). J Clin Oncol 2019;37:9011.
22. Drilon A, Cho BC, Kim D-W, Lee J, Lin JJ, Zhu V, et al. Safety and preliminary clinical activity of repotrectinib in patients with advanced ROS1/TRK fusion-positive solid tumors (TRIDENT-1 study). Ann Oncol 2019;30:159–93.
23. Soria JC, Ohe Y, Vansteenkiste J, Reungwetwattana T, Chewaskulyong B, Lee KH, et al. Osimertinib in untreated EGFR-mutated advanced non-small-cell lung cancer. N Engl J Med 2018;378:113–25.
24. Peters S, Camidge DR, Shaw AT, Gadgeel S, Ahn JS, Kim DW, et al. Alectinib versus crizotinib in untreated ALK-positive non-small-cell lung cancer. N Engl J Med 2017;377:829–38.
25. Yoda S, Lin JJ, Lawrence MS, Burke BJ, Friboulet L, Langenbucher A, et al. Sequential ALK inhibitors can select for lorlatinib-resistant compound ALK mutations in ALK-positive lung cancer. Cancer Discov 2018;8:714–29.

Published OnlineFirst April 8, 2020; DOI: 10.1158/1078-0432.CCR-19-2777

Clinical Cancer Research

Repotrectinib Exhibits Potent Antitumor Activity in Treatment-Naïve and Solvent-Front –Mutant ROS1-Rearranged Non–Small Cell Lung Cancer

Mi Ran Yun, Dong Hwi Kim, Seok-Young Kim, et al.

Clin Cancer Res 2020;26:3287-3295. Published OnlineFirst April 8, 2020.